

HVDC Modelling Requirements for Transient Stability Analyses of Large HVDC-AC Grids

Ahmed Mostafa Khalil *and* Reza Iravani

Abstract-- This paper introduces a systematic method to identify AC-fault locations within an HVDC-AC grid for which transient stability analysis of the overall system based on conventional active/reactive power (PQ) injection model of each HVDC station is not accurate and thus a more detailed model of the HVDC subsystem is required. Such locations (buses) constitute “Internal Zone(s)” and the rest, for which the active/reactive power injection model of HVDC subsystem is adequately accurate, construct “External Zone”. This categorization ensures accuracy of transient stability analyses and minimizes time/resource requirement for transient stability studies of large HVDC-AC grids. This paper demonstrates, in contrast to the widely used/adopted approach, that (i) Internal Zone is not necessarily restricted to the AC buses in electrical proximity of the HVDC grid and (ii) indiscriminate use of the conventional PQ-injection model of HVDC grid for all AC fault locations can result in erroneous transient stability analysis results. Feasibility and performance of the proposed method are evaluated by PSCAD-based time-domain simulation studies of a modified version of IEEE 39-Bus system which embeds a five-terminal MMC-based VSC-HVDC grid.

Keywords: HVDC Grid, Power systems dynamics, Frequency deviation, Measurement-based, Time-frequency analysis

I. INTRODUCTION

TECHNICAL and economical viability of the IGBT-based Voltage-Sourced Converter (VSC) technology, and specifically those of the Modular Multiterminal Converter (MMC) configuration [1, 2] has resulted in the emergence of HVDC-grid concept and applications [3, 4]. An HVDC grid is composed of multiple VSC-based HVDC converter stations, i.e., four or more [5], which at the DC-side are connected by a network of DC overhead lines and/or DC cables. The HVDC grid is interfaced with the host interconnected AC system (subsystems) at the converters’ AC-sides and enables:

- rapid and controllable power exchange among specific nodes without causing congestion/loop-flow [6], and/or
- controlled power transfer from multiple sources, e.g., wind and/or solar power plants, to the host AC grid [7, 8].

Time-domain Transient Stability (TS) analysis associated with low-frequency dynamics (0–2 Hz) of the HVDC-AC grid, is needed to identify system instability conditions/limits and determine appropriate control actions [9–11]. However, (i) rapid response of the HVDC grid control to a fault in its host AC system and (ii) major impact of HVDC grid on the post-fault power flow of the HVDC-AC system, indicate that classical TS component models do not accurately represent the

HVDC-AC low-frequency dynamics [12–16]. This is the impetus for more detailed representation of the HVDC-AC grid [12–16] for (i) TS studies subsequent to large disturbances [17–19] and (ii) security evaluation [20].

The technical literature reports two approaches for TS analyses of HVDC-AC grids:

- 1) Time-domain simulation of the overall system using Electro-Magnetic Transients (EMT) type models [18–21] of the HVDC grid and the host AC network. EMT-type models provide more detailed representations of the system apparatus as compared with their TS-type counterpart models. However, the required computational time and resources render this approach inapplicable to large, realistic-size HVDC-AC grids.
- 2) Hybrid time-domain simulation [22] which uses (i) EMT-type models for HVDC grid and (ii) classical TS-type models for AC network. This method requires an interface environment [23] between EMT-type and TS-type models [24].

The main limitation of the latter approach is that AC system disturbances close to HVDC stations result in inaccurate (erroneous) responses [25]. This is largely resolved by more detailed representation of a portion of the AC system, in vicinity of each HVDC station, i.e., EMT-type models instead of classical TS-type models [25]. The main drawback of this approach is the lack of a systematic method to identify that portion (zone) of the AC system to be represented by EMT-type models.

This paper introduces a method to systematically identify that part of the AC system to be represented by EMT-type models and defines the boundary between EMT-type and TS-type models of the AC system. The method, as shown in Fig.1, divides the AC network of an HVDC-AC system into External Zone (EZ) and Internal Zone (IZ) with the following features.

- For TS analysis of the overall HVDC-AC grid, subsequent to a large-signal disturbance in the EZ: (i) HVDC grid can be modelled by constant active/reactive (PQ) power injection at the AC-side of each HVDC converter station and (ii) apparatus in EZ can be represented by their conventional TS models. This is the de facto modeling approach as adopted by production-grade TS analysis software tools.
- For TS analysis of the overall HVDC-AC grid, subsequent to a large-signal disturbance in IZ, representation of HVDC grid, HVDC controls and IZ apparatus by their conventional TS models leads to erroneous results and more detailed models, e.g., EMT-type models [12–16], must be used. This modelling approach, although extensively discussed, has not been incorporated in production-grade TS analysis software

A. Khalil is with Electrical Power and Machines Department, Cairo University, Cairo, Egypt and also with Department of Electrical and Computer Engineering, University of Toronto, Toronto, Canada (e-mail: ahmed.khalil@ieec.org).

R. Iravani is with Department of Electrical and Computer Engineering, University of Toronto, Toronto, Canada (e-mail: iravani@ecf.utoronto.ca).

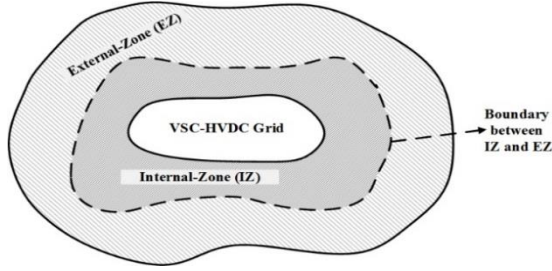


Fig. 1. Internal Zone (IZ) and External Zone (EZ) of an HVDC-AC system

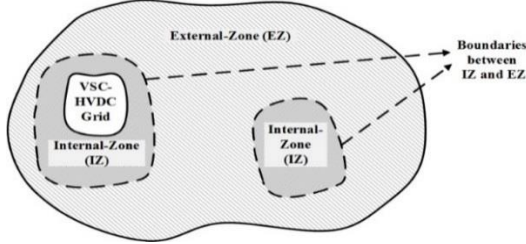


Fig. 2. Multiple Internal Zones of an HVDC-AC system

tools and the main reason is that the boundary between IZ and EZ cannot be systematically identified. This paper presents a method to identify the boundary nodes between IZ and EZ.

In contrast to the widely accepted belief, this paper also shows that IZ is not necessarily confined to the immediate area that surrounds the HVDC grid as shown in Fig. 1 but may also include other areas of the AC system, as shown in Fig. 2. This observation contradicts general intuition that large-signal disturbances of the AC system at remote nodes, with respect to HVDC grid stations, are of lesser impacts as compared to impacts of nodes which are electrically closer.

For separation of IZs and EZ, this paper proposes a clustering approach based on averaged-frequency deviation technique [26, 27] and we refer to it as Zone Identification Method (ZIM). The concept of Wide Area Monitoring System (WAMS) [27] is adopted in this paper to determine frequency deviations of AC buses. This paper applies ZIM to a modified version of the IEEE 39-bus system [28] that embeds a five-terminal MMC-based VSC-HVDC grid and also evaluates impacts of measurement white noise and simulation time-window on ZIM results.

This paper is organized as follows. Section II presents mathematical formulation of ZIM. Section III introduces the study system. Section IV applies ZIM to the study system and Section V concludes the paper.

II. ZONE IDENTIFICATION METHOD (ZIM)

Figure 2 shows that ZIM divides the AC subsystem of the HVDC-AC grid into two types of zones, i.e., EZ and IZ, and IZ is not necessarily confined to the AC power circuit surrounding the HVDC grid. The main contribution of this paper is development of ZIM to systematically identify the boundary between IZ and EZ as follows.

Consider the HVDC-AC grid of Fig. 3 and assume the AC grid is subjected to a large-signal disturbance, e.g., a fault (and its subsequent switching events) at AC bus “ j ”. For ZIM to determine if bus “ j ” is within EZ (or IZ), the low-frequency

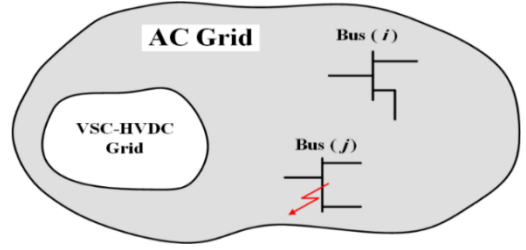


Fig. 3. Generic Representation of an HVDC-AC system

dynamic behavior of the HVDC-AC grid of Fig. 3 is investigated by two distinct representations of the HVDC grid:

- Representation-1: The HVDC grid is represented by (i) HVDC converter dynamic model, i.e., the averaged-model [14-16] or the switching-model [12-13], (ii) DC-line dynamic model, (iii) dynamic models of energy storage elements within the DC network and (iv) dynamic model of HVDC controls [12-16].
- Representation-2: The HVDC grid is modeled as a constant PQ-injection at each converter station, corresponding to the system steady-state operating point prior to the disturbance.

Frequency-deviation vector of bus “ i ” corresponding to Representation-1, owing to the AC grid disturbance at AC bus “ j ”, i.e., Δf_i^{j-1} , is constructed as

$$\Delta f_i^{j-1} = [\dots \Delta f_i^{j-1}|_{t-\Delta t}, \Delta f_i^{j-1}|_t, \Delta f_i^{j-1}|_{t+\Delta t} \dots]^T, \quad (1)$$

where t is time and Δt is the time-step for calculation of frequency deviation. Frequency deviation measurement ($\Delta f_i^{j-1}|_{t+\Delta t}$) is determined with respect to the steady-state system nominal frequency, i.e., f_0 (50 or 60Hz), from the rate of change of voltage phase-angle of bus “ i ”, i.e., θ_i^{j-1} , where

$$\Delta f_i^{j-1}|_{t+\Delta t} = \frac{1}{2\pi f_0} \left(\frac{\theta_i^{j-1}|_{t+\Delta t} - \theta_i^{j-1}|_t}{\Delta t} \right). \quad (2)$$

Number of entries of frequency-deviation vector Δf_i^{j-1} is

$$n = \frac{T}{\Delta t}, \quad (3)$$

where T is a predetermined simulation time-window subsequent to the disturbance. Similarly, for Representation-2, using the same disturbance, Δt and T , we determine frequency-deviation vector Δf_i^{j-2} . We define Closeness Coefficient CC_i^j of vectors Δf_i^{j-1} and Δf_i^{j-2} as the cosine of the angle between them,

$$CC_i^j = \frac{\Delta f_i^{j-1T} \Delta f_i^{j-2}}{\|\Delta f_i^{j-1}\| * \|\Delta f_i^{j-2}\|}. \quad (4)$$

CC_i^j varies from -1 to 1 where $CC_i^j = 1$ indicates identical Δf_i^{j-1} and Δf_i^{j-2} and thus concludes the same dynamical responses corresponding to Representation-1 and Representation-2. Based on CC_i^j , we introduce Response Closeness Index (RCI), for each of Representation-1 and Representation-2, corresponding to the disturbance at bus “ j ”, i.e.,

$$RCI_j = \sqrt{\frac{\sum_{i=1}^N (CC_i^j)^2}{N}}, \quad (5)$$

where N is the number of AC buses of the system. RCI_j is the root-mean-square value of the closeness coefficients calculated at all AC buses associated with the disturbance at bus “ j ”. RCI_j provides a measure to determine if Representation-1, i.e., a more detailed HVDC grid model, is necessary to investigate the HVDC-AC grid dynamics owing to the disturbance at bus “ j ”. RCI_j varies from 0 to 1 where

- $RCI_j = 1$ indicates the two HVDC grid representations provide identical responses owing to the disturbance at bus “ j ”.
- $RCI_j = 0$ indicates the two HVDC grid representations result in different responses and thus the HVDC grid dynamics cannot be ignored, and the more detailed model of the HVDC grid is required.

Based on a selected closeness limit γ , e.g., $\gamma = 0.9$, bus “ j ” is admitted to either IZ or EZ as follows. If

$$RCI_j > \gamma \leftrightarrow Bus\ j \in EZ, \quad (6)$$

then Representation-1 and Representation-2 provide adequately “close” responses at bus “ j ” and the PQ-injection model adequately represents the HVDC grid and bus “ j ” is admitted to EZ. To the contrary, if

$$RCI_j < \gamma \leftrightarrow Bus\ j \in IZ, \quad (7)$$

then responses corresponding to Representation-1 and Representation-2 are not “close”. Thus, Representation-1 must be used to obtain adequately accurate results and PQ-model is not an accurate representation. Therefore, bus “ j ” is admitted to IZ. Selecting a larger (smaller) γ reduces (increases) the number of buses in EZ and thus makes IZ larger (smaller). It should be noted that ZIM is only applicable to disturbances at AC buses and not to DC network faults.

III. STUDY SYSTEMS

A modified version of the IEEE 39-bus system [28], as shown in Fig. 4, is used to demonstrate applications of ZIM. In the system of Fig. 4:

- Power ratings of generators (and transformers) are kept the same as those of [29] except for Gen-2 and Gen-3 (and their transformers) which are doubled. The set points for Gen-2 and Gen-3 are increased to 1000 MW and 1150 MW, respectively;
- Loads at Bus-4 and Bus-8 are increased from 500 MW and 522 MW to 1000 MW and 1000 MW, respectively;
- One AC transmission line is added between Bus-4 and Bus-11;
- Bus-11 and Bus-13 are tied to prevent circulating current of transformers connected to Bus-12.

The above changes result in congestion in the shaded area of Fig. 4. This is addressed by replacing the shaded area by a five-terminal, mono-polar, MMC-based VSC-HVDC grid [30] as shown in Fig. 5. The nominal DC grid voltage is 640kV. Each MMC is connected to the corresponding AC bus through a Y/ Δ transformer [31]. MMC-3 controls the DC voltage and

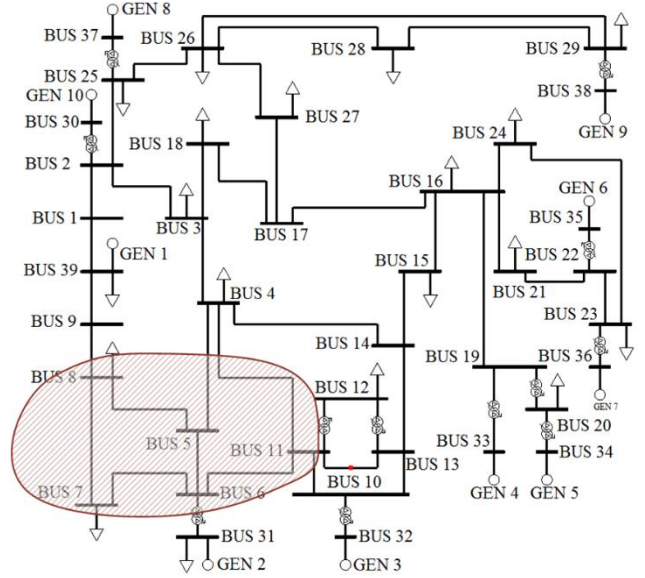


Fig. 4. Single-line diagram of the original AC system

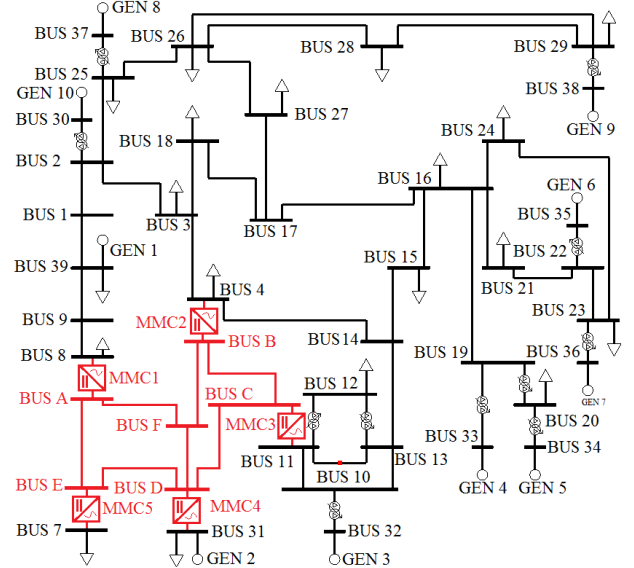


Fig. 5. Single-line diagram of HVDC-AC system (and Representation-1)

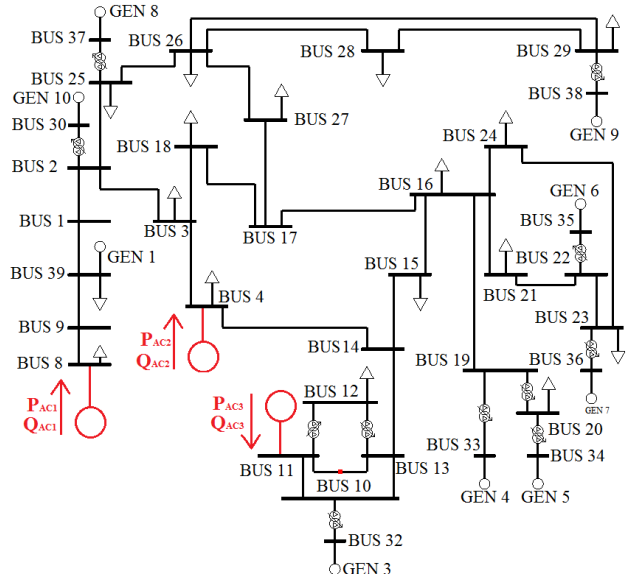


Fig. 6. Single-line diagram of HVDC-AC system (and Representation-2)

TABLE I – STEADY-STATE OPERATING POINT OF MMCs

MMC	1	2	3
Active Power (MW)	-943.7	-684.6	912.2
Reactive Power (MVar)	-79.4	-36	63.47

the other MMCs regulate power exchange between corresponding AC and DC buses. MMC-5 supplies a passive system and MMC-4 is connected to a source, i.e., equivalent of a wind power plant [28]. Details of the HVDC grid and its parameters are given in [30]. The HVDC grid is equipped with an enhanced dead-band-based, DC voltage droop-control for each converter station [30].

Figure 6 shows the system of Fig. 5 in which the HVDC grid is represented by equivalent constant PQ-injections at HVDC stations corresponding to MMC-1, MMC-2 and MMC-3. MMC-4 and MMC-5 stations are not identified in Fig. 6 since their AC buses are isolated from the AC network. Therefore, Bus-7 and Bus-31 of Fig. 4 are not shown in Fig. 6. The constant PQ-injections of MMC-1 to MMC-3 are obtained from the system power flow analysis as given in Table I

IV. STUDY RESULTS

The objectives of the study cases are to (i) illustrate that PQ-injection model (Representation-2) of HVDC system can result in erroneous TS analysis results of HVDC-AC system and (ii) demonstrate application of ZIM to identify the boundaries between IZ and EZ for Representation-1 for TS studies. The studies are conducted on the systems of Fig. 5 and Fig. 6.

Case-I

Figure 7 shows frequency deviation signals at Bus-14 of the system of Fig. 5 (Representation-1) due to a 5-cycle, self-cleared, 3-phase fault at Bus-9. For each turbine-generator unit (i) rotor mechanical system is modeled based on its single-mass representation and (ii) governor and excitation systems are modelled based on GOV1, IEEE DC1A respectively [28]. Each MMC is represented by the model of [31] where each sub-module contains a capacitor and two IGBT switch cells. For each MMC unit, transformer leakage inductance, arm inductance, sub-module capacitor, and DC line parameters are adopted from [28]. Details of VSC-HVDC grid control are given in [30]. Figure 7 clearly shows the fault results in damped low-frequency electromechanical dynamics and subsequently the dynamic response is dominated by high-frequency oscillations owing to the switching model of MMC stations which are electrically close to Bus14.

Figure 7 also shows the system response to the same fault under the same operating conditions when the HVDC system is modelled by PQ-injection (Representation-2) as illustrated in Fig. 6. Comparison of responses corresponding to Representation-1 and Representation-2 clearly shows that PQ-injection model of Representation-2 provide unrealistic (erroneous) results, particularly immediately after the fault inception.

Case-II

Figure 8 shows frequency deviation signals at Bus-28 and

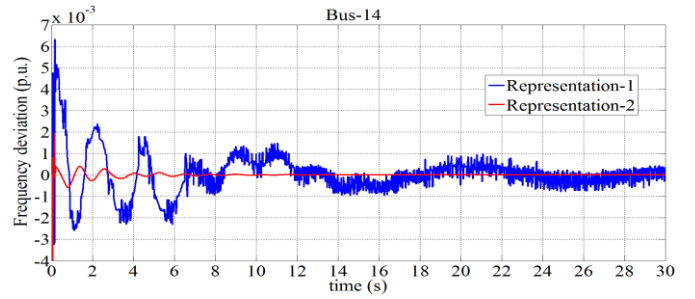


Fig. 7. Frequency deviation signals due to the fault at BUS-9

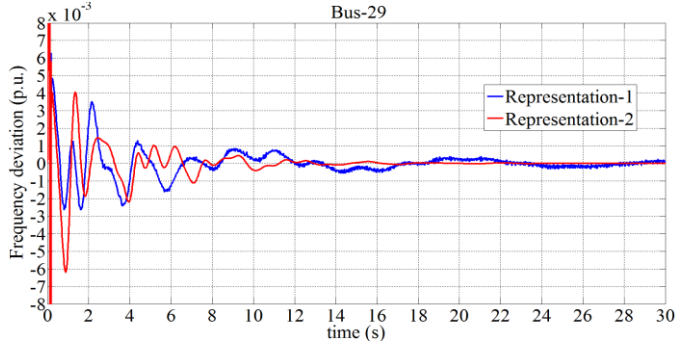
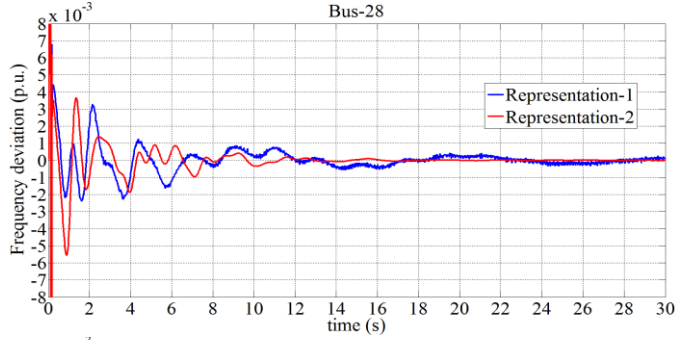


Fig. 8. Frequency deviation signals due to the fault at BUS-26

Bus-29, in response to the fault of Case-I at Bus-26, corresponding to Representation-1 (Fig. 5) and Representation-2 (Fig. 6). As compared with Fig. 7, Fig. 8 indicates the corresponding responses of Representation-1 and Representation-2 are practically close and thus PQ-injection model is a valid representation of the HVDC system for TS studies. Figures 7 and 8 demonstrate that faulted Bus-9 (corresponding to Fig. 7) and Bus-26 (corresponding to Fig. 8) belong to IZ and EZ respectively. The proposed method of Section-II can systematically allocate the faulted AC buses in either IZ or EZ and identify appropriate representation for TS studies, as follows.

Case-III

To identify whether an AC bus is in IZ or EZ, (1-3) are used to construct its frequency-deviation vectors corresponding to Representation-1 and Representation-2. An M-class Phasor Measurement Unit (PMU) [32, 33] at each AC bus is used for frequency measurements. The time response of each PMU is (i) filtered by a Finite Impulse Response (FIR) filter and (ii) reported at the rate of 60 Hz ($\Delta t = 16.67$ ms in (3)).

Based on the frequency-deviation vectors, RCI values from (5) are calculated and shown in Fig. 9. The lowest and highest RCI values of Fig. 9 are 0.414 and 0.99 which correspond to Bus-9 and Bus-17 respectively. Bus-9 is directly connected to

Bus-8, i.e., AC interface bus of MMC-1 (Fig. 5). Therefore, the system response to a fault at Bus-9 is highly affected by MMC-1 model as identified by its low RCI value of 0.414 and illustrated and verified by Fig. 7.

Highest RCI value of Fig. 9 belongs to Bus-17 which is remote from and weakly coupled to the HVDC grid and generators. This highlights that a fault at Bus-17 results in insignificant changes of voltages of AC generators and MMC AC sides. Thus, Bus-17 is in EZ and Representation-2, i.e., PQ-injection model, adequately models the HVDC system for TS studies subsequent to a fault at Bus-17. Wide range of variations of RCI values of Fig. 9 reveals that if Representation-1 is adopted for TS studies at each AC bus, the computational burden will be unnecessarily significant.

Figure 9 also indicates small RCI=0.72 for Bus-1. The reason is that Bus-1 is directly connected to GEN-1 which represents an equivalent area and the fault at Bus-1 excites GEN-1 local oscillatory mode. Thus, the voltage of Bus-8, which is connected to Bus-1 through a radial line, significantly decreases and power exchange between MMC-1 and AC network drastically changes. This indicates detailed representation of MMC-1 is needed for TS studies for a fault on Bus-1.

Figure 9 shows that RCI values of Bus-26 to Bus-29 are very large. The reasons are (i) Bus-26 to Bus-29 are weakly tied to the remaining part of the HVDC-AC system and (ii) electrically remote from the MMC stations. Therefore, faults at these buses result in relatively small changes in AC-side voltages of MMCs and power exchange between the HVDC grid and the AC network remains nearly unchanged. Therefore, Representation-2, i.e., PQ-injection model, adequately represents the HVDC system as illustrated in Fig. 8 and numerically expressed by RCI values of Fig. 9.

Figure 10 pictorially shows the EZ and IZ locations on the study system corresponding to closeness limit of $\gamma=0.9$ and also highlights that the study system contains two IZs. Existence of two IZs in Fig. 10 is counterintuitive, i.e., for TS studies subsequent to faults at remote Bus-21 to Bus-24 of Fig. 10, simplified PQ-model of HVDC grid is not acceptable. The general assumption is that the PQ-injection model of HVDC system is valid for TS studies subsequent to faults at electrically remote buses with respect to the HVDC stations. The proposed ZIM shows that this intuitive assumption is not valid. The physical reasoning is that integration of HVDC grid drastically alters pattern and/or dampings of low-frequency dynamics of the original host AC system [28]. Reference [28] highlights that embedding an HVDC grid in an AC system, without appropriate provisions, e.g., supplementary HVDC controls, can increase propensity of the AC system to low-frequency oscillations.

To show the benefits of the proposed method, the decrease in the computational burden is investigated. Table II shows CPU-time for 60 seconds time-domain simulation of the study system subsequent to the fault on Bus-16 using Representation-1 (Fig. 5) and Representation-2 (Fig.6) for the HVDC grid. An Intel® Core™ i5-3210M 2.5GHz computer with 4GB of memory is used for the simulation studies (simulation time-step of 50 μ s). Table II shows that CPU-time based on Representation-2 is one order of magnitude smaller than that of Representation-1 while the corresponding results

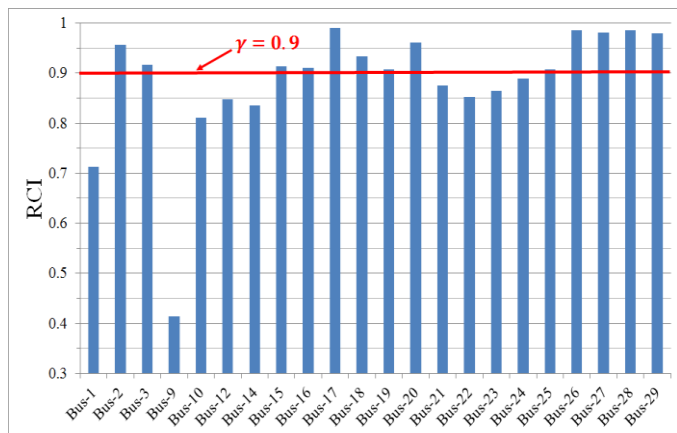


Fig. 9. RCIs of AC buses of the study system

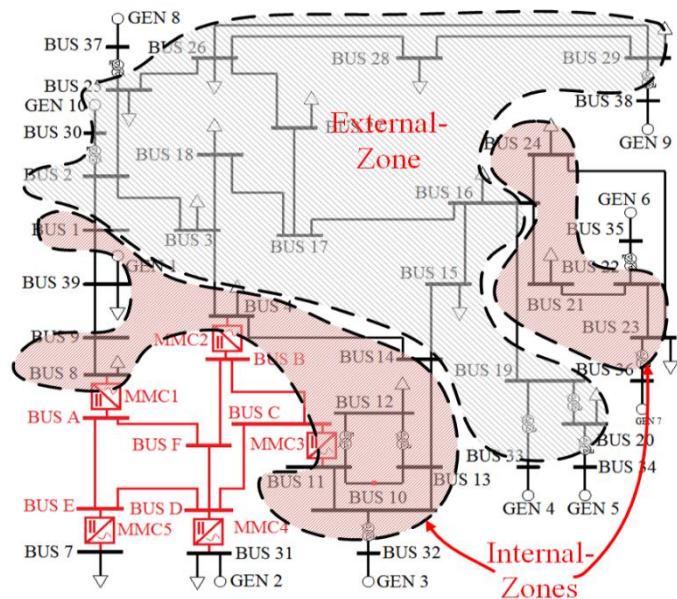


Fig. 10. EZ and IZ of the HVDC-AC system

TABLE II – CPU-TIME FOR FAULT AT BUS-16 BASED ON REPRESENTATION-1 AND REPRESENTATION-2 OF THE HVDC GRID

	Representation-1	Representation-2
CPU-time (seconds)	3767.23	368.70

closely agree. This clearly shows that ZIM can systematically identify disturbance locations for which Representation-2 of the HVDC grid can provide the same degree of accuracy as that of Representation-1 while significantly reducing CPU-time.

V. CONCLUSIONS

This paper introduces, develops and evaluates a Zone Identification Method (ZIM) to systematically locate AC buses into External Zone (EZ) and Internal Zone (IZ) of an AC system which embeds an HVDC grid. For transient stability (TS) analysis of the overall system, subsequent to faults within EZ, the HVDC grid can be accurately represented by active/reactive (PQ) injection at HVDC converter stations. However, IZ consists of AC buses where TS analysis of the overall system requires detailed models of

the HVDC grid and its controls, and PQ-injection model is not applicable. The proposed ZIM is an off-line approach which divides the system into EZ and IZ based on frequency-deviation signals of AC buses subsequent to faults.

The paper applies ZIM to a modified version of the IEEE 39-bus system embedding a five-terminal MMC-based VSC-HVDC grid and evaluates its feasibility and sensitivity to measurement noise and size of frequency-deviation vectors. The study results conclude:

- ZIM is an effective tool to decrease computation time of TS studies and analyses of low-frequency dynamics, e.g., coherency and inter-area oscillation phenomena, of HVDC-AC grids by appropriate selection of HVDC grid model for each AC-bus fault. The time saving for fault studies of specific buses can be one order of magnitude.
- ZIM reveals that, depending on the dynamic characteristics of the HVDC-AC system, (i) IZ can encompass multiple distinct areas, (ii) IZ is not necessarily limited to AC buses in immediate/close vicinity of the HVDC grid and (iii) electrically remote AC buses from the HVDC grid also can form an IZ.
- ZIM eliminates the guess-work of the decision-making process to identify that portion of AC system which requires more detailed representation for TS studies.

VI. REFERENCES

- [1] A. Lesnicar and R. Marquardt, "An innovative modular multilevel converter topology suitable for a wide power range," in Proc. IEEE Power Tech. Conf., Bologna, Italy, Jun. 2003, pp. 1–6.
- [2] G. Ding, G. Tang, Z. He, and M. Ding, "New technologies of voltage source converter (VSC) for HVDC transmission system based on VSC," in Proc. IEEE Power Eng. Soc. Gen. Meeting, Beijing, China, Jun. 2008, pp. 1–8.
- [3] CIGRE Technical Brochure "HVDC Grid Feasibility Study" Working Group 52 of Study Committee B4, April 2013
- [4] D. V. Hertem, O. Gomis-Bellmunt, J. Liang, HVDC Grids: For Offshore and Supergrid of the Future. Piscataway, NJ, USA: IEEE/Wiley, 2016
- [5] CIGRE Technical Brochure "VSC Transmission" Working Group 37 of Study Committee B4, April 2005
- [6] N. R. Chaudhuri, B. Chaudhuri, R. Majumder, and A. Yazdani, Multiterminal Direct-Current Grids: Modeling, Analysis, and Control. Piscataway, NJ, USA: IEEE/Wiley, 2014
- [7] J. Liang, T. Jing, O. Gomis-Bellmunt, J. Ekanayake, N. Jenkins, "Operation and control of multiterminal HVDC transmission for offshore wind farms," in *IEEE Transactions on Power Delivery*, vol. 26, no. 4, pp. 2596-2604, Oct. 2011.
- [8] S. A. Amamra, F. Colas, X. Guillaud, P. Rault and S. Nguefeu, "Laboratory Demonstration of a Multiterminal VSC-HVDC Power Grid," in *IEEE Transactions on Power Delivery*, vol. 32, no. 5, pp. 2339-2349, Oct. 2017.
- [9] J. Renedo; A. García-Cerrada; L. Rouco, "Active Power Control Strategies for Transient Stability Enhancement of AC/DC Grids With VSC-HVDC Multi-Terminal Systems," in *IEEE Transactions on Power Systems*, vol. 31, no. 6, pp. 4595-4604, Nov. 2016.
- [10] S. Liu, Z. Xu, W. Hua, G. Tang, and Y. Xue, "Electromechanical transient modeling of modular multilevel converter based multiterminal HVDC system," *IEEE Trans. Power Syst.*, vol. 29, no. 1, pp. 72–83, Jan. 2014.
- [11] L. Shen, M. Barnes, R. Preece, J. V. Milanovic, K. Bell and M. Belivanis, "The Effect of VSC-HVDC Control on AC System Electromechanical Oscillations and DC System Dynamics," in *IEEE Transactions on Power Delivery*, vol. 31, no. 3, pp. 1085-1095, June 2016. DOI: 10.1109/TPWRD.2015.2414824
- [12] U. N. Gnanarathna, A. M. Gole, and R. P. Jayasinghe, "Efficient modeling of modular multilevel HVDC converters (MMC) on electromagnetic transient simulation programs," *IEEE Trans. Power Del.*, vol. 26, no. 1, pp. 316–324, Jan. 2011.
- [13] P. Le-Huy, P. Giroux, and J.-C. Soumagne, "Real-time simulation of modular multilevel converters for network integration studies," presented at the Int. Conf. Power Syst. Transients, Delft, the Netherlands, Jun. 14–17, 2011.
- [14] W. Yang, Q. Song and W. Liu, "Decoupled Control of Modular Multilevel Converter based on Intermediate Controllable Voltages," in *IEEE Transactions on Industrial Electronics*, vol. 63, no. 8, pp. 4695-4706, Aug. 2016
- [15] J. Peralta, H. Saad, S. Denetiere, and J. Mahseredjian, "Dynamic performance of average-value models for multi-terminal VSC-HVDC systems," IEEE Power Eng. Soc. Gen. Meeting, San Diego, CA, 2012.
- [16] J. Peralta, S. Denetiere, and J. Mahseredjian, "Average-value models for the simulation of VSC-HVDC transmission systems," in Proc. CIGRE Bologna Symp., Bologna, Italy, Sep. 13–15, 2011.
- [17] L. Tang and B. T. Ooi, "Locating and Isolating DC Faults in Multi-Terminal DC Systems," in *IEEE Transactions on Power Delivery*, vol. 22, no. 3, pp. 1877-1884, July 2007.
- [18] J. Yang, J. E. Fletcher and J. O'Reilly, "Short-Circuit and Ground Fault Analyses and Location in VSC-Based DC Network Cables," in *IEEE Trans. on Industrial Elect.*, vol. 59, no. 10, pp. 3827-3837, Oct. 2012.
- [19] J. Renedo, A. García-Cerrada and L. Rouco, "Active Power Control Strategies for Transient Stability Enhancement of AC/DC Grids With VSC-HVDC Multi-Terminal Systems," in *IEEE Transactions on Power Systems*, vol. 31, no. 6, pp. 4595-4604, Nov. 2016.
- [20] H. Saad *et al.*, "Dynamic Averaged and Simplified Models for MMC-Based HVDC Transmission Systems," in *IEEE Transactions on Power Delivery*, vol. 28, no. 3, pp. 1723-1730, July 2013.
- [21] S. Liu, Z. Xu, W. Hua, G. Tang and Y. Xue, "Electromechanical Transient Modeling of Modular Multilevel Converter Based Multi-Terminal HVDC Systems," in *IEEE Transactions on Power Systems*, vol. 29, no. 1, pp. 72-83, Jan. 2014.
- [22] F. Plumier, P. Aristidou, C. Geuzaine and T. Van Cutsem, "Co-Simulation of Electromagnetic Transients and Phasor Models: A Relaxation Approach," in *IEEE Transactions on Power Delivery*, vol. 31, no. 5, pp. 2360-2369, Oct. 2016.
- [23] Jalili-Marandi, V. Dinavahi, K. Strunz, J. A. Martinez and A. Ramirez, "Interfacing Techniques for Transient Stability and Electromagnetic Transient Programs IEEE Task Force on Interfacing Techniques for Simulation Tools," in *IEEE Transactions on Power Delivery*, vol. 24, no. 4, pp. 2385-2395, Oct. 2009.
- [24] D. Shu, X. Xie, Q. Jiang, Q. Huang and C. Zhang, "A Novel Interfacing Technique for Distributed Hybrid Simulations Combining EMT and Transient Stability Models," in *IEEE Transactions on Power Delivery*, vol. 33, no. 1, pp. 130-140, Feb. 2018.
- [25] D. Shu *et al.*, "Dynamic Phasor Based Interface Model for EMT and Transient Stability Hybrid Simulations," in *IEEE Transactions on Power Systems*, vol. 33, no. 4, pp. 3930-3939, July 2018
- [26] A. Mohammed, "Impacts of High-Depth of Penetration of Wind Power on Interconnected Power Systems Dynamics," Ph.D. dissertation, Elect. and Comp. Eng. Dept., Univ. Toronto, Toronto, 2016.
- [27] A. M. Khalil and R. Iravani, "A Dynamic Coherency Identification Method Based on Frequency Deviation Signals," in *IEEE Transactions on Power Systems*, vol. 31, no. 3, pp. 1779-1787, May 2016.
- [28] F. B. Ajaei and R. Iravani, "Dynamic Interactions of the MMC-HVDC Grid and its Host AC System Due to AC-Side Disturbances," in *IEEE Trans. on Power Delivery*, vol. 31, no. 3, pp. 1289-1298, June 2016.
- [29] T. B. Nguyen and M. A. Pai, "Dynamic security-constrained rescheduling of power systems using trajectory sensitivities," *IEEE Trans. Power Syst.*, vol. 18, no. 2, pp. 848–854, May 2003.
- [30] H. Li, C. Liu, G. Li and R. Iravani, "An Enhanced DC Voltage Droop-Control for the VSC-HVDC Grid," in *IEEE Transactions on Power Systems*, vol. 32, no. 2, pp. 1520-1527, March 2017.
- [31] J. Peralta, H. Saad, S. Denetiere, J. Mahseredjian, and S. Nguefeu, "Detailed and averaged models for a 401-level MMC-HVDC system," *IEEE Trans. Power Del.*, vol. 27, no. 3, pp. 1501–1508, Jul. 2012.
- [32] IEEE Standard for Synchrophasor Measurements for Power Systems," in *IEEE Std C37.118.1-2011 (Revision of IEEE Std C37.118-2005)*, vol., no., pp.1-61, Dec. 28
- [33] Standard for Synchrophasor Measurements for Power Systems -- Amendment 1: Modification of Selected Performance Requirements," in *IEEE Std C37.118.1a-2014 (Amendment to IEEE Std C37.118.1-2011)* vol., no., pp.1-25, April 30, 2014